Journal of Applied Electrochemistry (2006) 36:991–996
DOI 10.1007/s10800-006-9129-8

Numerical optimization of bipolar plates and gas diffusion layers for PEM fuel cells

S.A. GRIGORIEV[1,*], A.A. KALINNIKOV[1], V.N. FATEEV[1] and A.A. WRAGG[2]
[1]*Hydrogen Energy and Plasma Technology Institute of Russian Research Center "Kurchatov Institute", Kurchatov sq., 1, 123182, Moscow, Russia*
[2]*Department of Engineering, University of Exeter, Exeter, EX4 4QF, UK*
*(*author for correspondence, fax: + 7-495-196-6278, E-mail: s.grigoriev@hepti.kiae.ru)*

Received 23 December 2004; accepted in revised form 23 January 2006

Key words: bipolar plate, gas diffusion layer, mathematical modelling, optimization, PEM fuel cells

Abstract

This paper is devoted to the numerical optimization of the dimensions of channels and current transfer ribs of bipolar plates as well as the thickness and porosity of gas diffusion layers. A mathematical model of the transfer processes in a PEM fuel cell has been developed for this purpose. The results are compared with experimental data. Recommendations of the values of operating parameters and some design requirements to increase PEM fuel cell efficiency are suggested.

Nomenclature (List of symbols)

d_r	Width of current transfer rib (mm)
d_c	Width of the gas channel (mm)
h	Gas diffusion layer thickness (mm)
ε	Gas diffusion layer porosity
n	Volumetric concentration of a reagent
n_o	Initial volumetric concentration of reagent
D_o	Diffusion coefficient of a reagent ($mm^2\ s^{-1}$)
D	Diffusion coefficient of a reagent in porous media ($mm^2\ s^{-1}$)
i	Current density ($A\ cm^{-2}$)
F	Faraday number (96487 $C\ mol^{-1}$)
U_{out}	Output voltage of fuel cell (V)
ϕ	Potential (V)
ρ_x, ρ_y	Specific electrical conductivity of gas diffusion layer in directions x and y, respectively ($S\ cm^{-1}$)
E_{eq}	Equilibrium potential (V)
R_{ef}	Effective electrical resistance of membrane and electrocatalytic layer ($\Omega\ cm^2$)
i_o	Exchange current density ($A\ cm^{-2}$)
p	Oxygen partial pressure (bar)
p_o	Reference oxygen pressure (bar)
α	Electron transfer coefficient
z	Number of electrons involved in the reaction
η	Overpotential (V)
R	Gas constant (8.3145 $J\ K^{-1}\ mol^{-1}$)
T	Absolute temperature (K)
ρ_o	Specific electric conductivity of carbon ($S\ cm^{-1}$)
t	Fuel cell temperature (°C)
Pair	Air pressure (bar)
PH_2	Hydrogen pressure (bar)

1. Introduction

Proton exchange membrane (PEM) fuel cells are being developed worldwide for vehicle, stationary and portable applications. Optimization of the fuel cell stack components such as bipolar plates and gas diffusion layers is one of the main tasks for PEM fuel cell engineering. For example, optimization of the dimensions of channels and current transfer ribs (the so-called flow-field) of bipolar plates, and also the thickness and porosity of gas diffusion layers, pose a significant problem [1–5]. Earlier, the authors developed a two-dimensional diffusion model of mass transfer processes in PEM fuel cells [6, 7]. This model showed that at specific operating current densities, diffusion limitations may occur in the gas diffusion layers. This work explores the problem further for gas diffusion layers of various structures and compositions taking into account ohmic losses and the sizes of channels and current transfer ribs of the bipolar plates.

2. Mathematical model

2.1. *Model description and assumptions*

A PEM fuel cell is a complex system whose performance is determined by the parameters of each individual component. Therefore, mathematical models that jointly consider the various processes in all the fuel cell components (see, for example, [8–10]) are highly useful. Within the two-dimensional mathematical model devel-

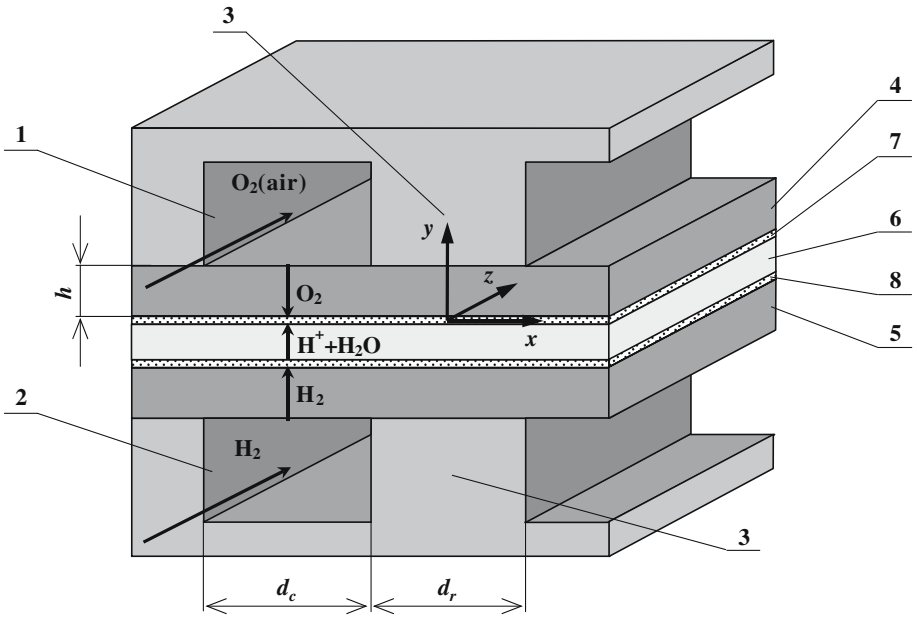

Fig. 1. Scheme of the cell components. 1 – cathode (air) channel, 2 – anode (hydrogen) channel, 3 – current transfer rib, 4 – cathode gas diffusion layer, 5 – anode gas diffusion layer, 6 – membrane, 7 – cathode electrocatalytic layer, 8 – anode electrocatalytic layer.

oped in the present study the assessment of the influence on current density of the bipolar plate and gas diffusion layer parameters, as well as the electrocatalytic layers and the membrane, is treated.

Figure 1 shows all the characteristic areas of a fuel cell. The model specifies these areas separately and they are related through boundary conditions. The model describes the following processes:

- transport of reagent and water in the bipolar plate channels, gas diffusion layers, electrocatalytic layers and in the membrane;
- the proton flux in the membrane and the electrocatalytic layer;
- the electronic current in the electrocatalytic and gas diffusion layers and current transfer ribs of the bipolar plate;
- heat transfer in all components.

The model involves the following basic assumptions:

- the gas in the bipolar plate channels is ideal and flows at constant pressure;
- there is no longitudinal component of gas speed (along the z axis) in a gas diffusion layer;
- the pressures in the cathode and anode zones are equal;
- all the mass transfer processes occur at constant pressure;
- the catalytic layer has negligible thickness;
- the contacting surfaces of the bipolar plates and the gas diffusion layers have identical temperatures and are equipotential.

2.2. *Governing equations and boundary conditions*

The Stephan–Maxwell equation was used to describe mass transfer in the bipolar plate channels and gas diffusion layers. The distribution of gas flow in the channels was described by means of the Navier–Stokes equation for quasi-steady flow. The proton flux in the membrane and electrocatalytic layer was calculated using the Nernst–Planck equation. Thermal processes were described through appropriate heat transfer equations.

When using a bipolar plate with a linear arrangement of channels and ribs (as for other types of bipolar plate) the surface of the electrocatalytic layer may not be equally accessible for a reagent transporting from the bipolar plate channels through the gas diffusion layers. Due to the increase in the diffusion length, additional diffusion limitations may occur for areas of electrocatalytic layer surface located opposite to current transfer ribs, contacting the gas diffusion layer (Figure 1). On the other hand, an increase in ohmic losses in the gas diffusion layer may occur in the areas above the channels.

An elemental section ''middle of rib to middle of channel'' (see Figure 1) was considered. Mass transfer in the porous gas diffusion layer was calculated using a second order equation:

$$D\frac{\partial^2 n}{\partial x^2} + D\frac{\partial^2 n}{\partial y^2} = 0. \tag{1}$$

The boundary conditions are

$$x = 0,\ 0yh : \frac{\partial n}{\partial y} = 0$$

$$x = \frac{d_r + d_c}{2},\ 0yh : \frac{\partial n}{\partial y} = 0$$

$$y = 0,\ 0x\frac{d_r + d_c}{2} :\ D\frac{\partial n}{\partial y} = \frac{i}{4F}$$

$$y = h,\ 0x < \frac{d_r}{2} :\ \frac{\partial n}{\partial y} = 0$$

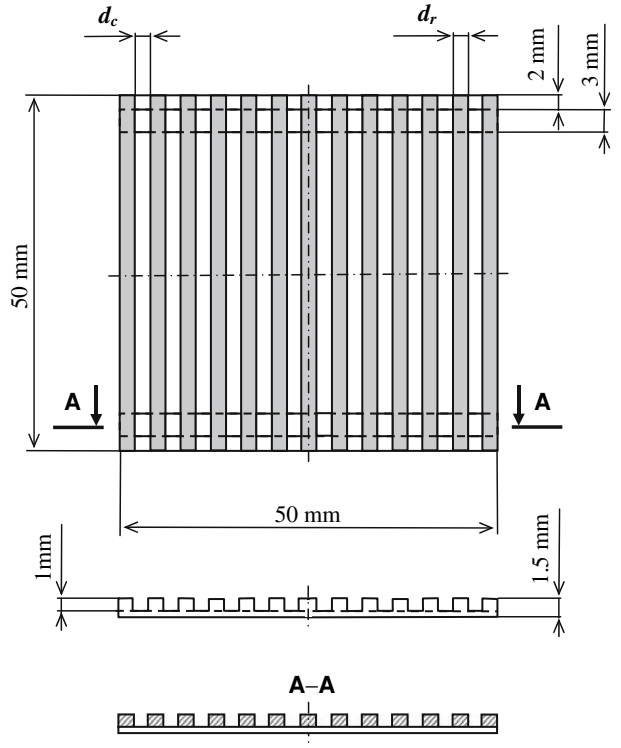

Fig. 2. Layout of air flow-field used in experiments.

$$y = h,\ \frac{d_r}{2}x < \frac{d_r + d_c}{2} :\ n = n_o.$$

The potential distribution in the gas diffusion layer was described by a similar equation:

$$\frac{1}{\rho_x}\frac{\partial^2\varphi}{\partial x^2} + \frac{1}{\rho_y}\frac{\partial^2\varphi}{\partial y^2} = 0. \tag{2}$$

The boundary conditions are

$$x = 0,\ 0yh :\ \frac{\partial\varphi}{\partial x} = 0$$

$$x = \frac{d_r + d_c}{2},\ 0yh :\ \frac{\partial\varphi}{\partial x} = 0$$

$$y = h,\ 0x < \frac{d_r}{2} :\ \varphi = U_{\text{out}}$$

$$y = h,\ \frac{d_r}{2}x < \frac{d_r + d_c}{2} :\ \frac{\partial\varphi}{\partial y} = 0.$$

The condition connecting potential and concentration of reagent in the electrocatalytic layer is

$$y = 0,\ 0x\frac{d_r + d_c}{2} :\ i = \frac{1}{\rho_y}\frac{\partial\varphi}{\partial y} = 4FD\frac{\partial n}{\partial y}.$$

Taking into consideration that $i = i_o\frac{p}{p_o}\exp\frac{\alpha zF\eta}{RT}$ (Tafel equation) and $\phi = E_{\text{eq}} - \eta - iR_{\text{ef}}$, the current density at the boundary between cathode electrocatalytic and gas diffusion layers is given by the following equation:

$$E_{\text{eq}} - \varphi - iR_{\text{ef}} = \frac{RT}{\alpha zF}\ln\frac{i}{i_o}\frac{p_o}{p} = 0. \tag{3}$$

To account for the influence of the gas diffusion layer porosity on the diffusion coefficient of a reagent and on electrical conductivity the following equations were used:

$$D = D_o\varepsilon^{1.5}$$

$$\rho = \rho_o(1 - \varepsilon)^{-1.5}.$$

Furthermore, the model accounts for the transport of water in the membrane and the electrocatalytic and gas diffusion layers. However, this item is beyond the scope of this article and will be published separately.

2.3. *Numerical technique*

In order to achieve a numerical (computational) solution, Equations (1)–(3) were transformed into a form convenient for solution by the relaxation method (we found a stable, steady state, solution of the similar unsteady-state equations). The unsteady-state equations were solved by a grid method. The numerical solution of each two-dimensional equation on the space grid was performed by means of the use of an alternating direction method.

The original software, developed by the authors, was applied for collateral numerical solution of the above system of equations by use of a grid method.

3. Experimental procedure

Experimental determination of the influence of channel and rib dimensions on the cathode side of a bipolar plate, and also the gas diffusion layer parameters on fuel cell performance was carried out for verification and modifications of the model. We used Nafion-112 perfluorinated ion-exchange polymer membrane for preparation of membrane–electrode assemblies. The catalyst was 40 wt% Pt on a hydrophobic carbon carrier (10% PTFE), the Pt loading at the anode and cathode was 0.35 mg cm^{-2}. The thickness of the gas diffusion layer was $h = 0.28$ mm, with effective porosity $\varepsilon = 0.7$.

Bipolar plates with different flow-field design were manufactured. Channels and ribs on the air side had a rectilinear structure and dimensions of 0.5–5.0 mm (see Figure 2). The height of the channels in all cases was 1 mm. Flow-field plates were made of stainless steel 12X18H10T. The hydrogen flow-field was represented by metal felt with a thickness of 2 mm.

In order to achieve a uniform supply of reactants, the flow-field had a distributed inlet/outlet arrangement. The operating area of the fuel cell was 25 cm^2. The hold-down clamping pressure was 50 kg cm^{-2}.

4. Results and discussion

4.1. *The effect of bipolar plate and gas diffusion layer parameters on current density*

The distributions of current density as a function of the geometric parameters of the cathode (air) side of the

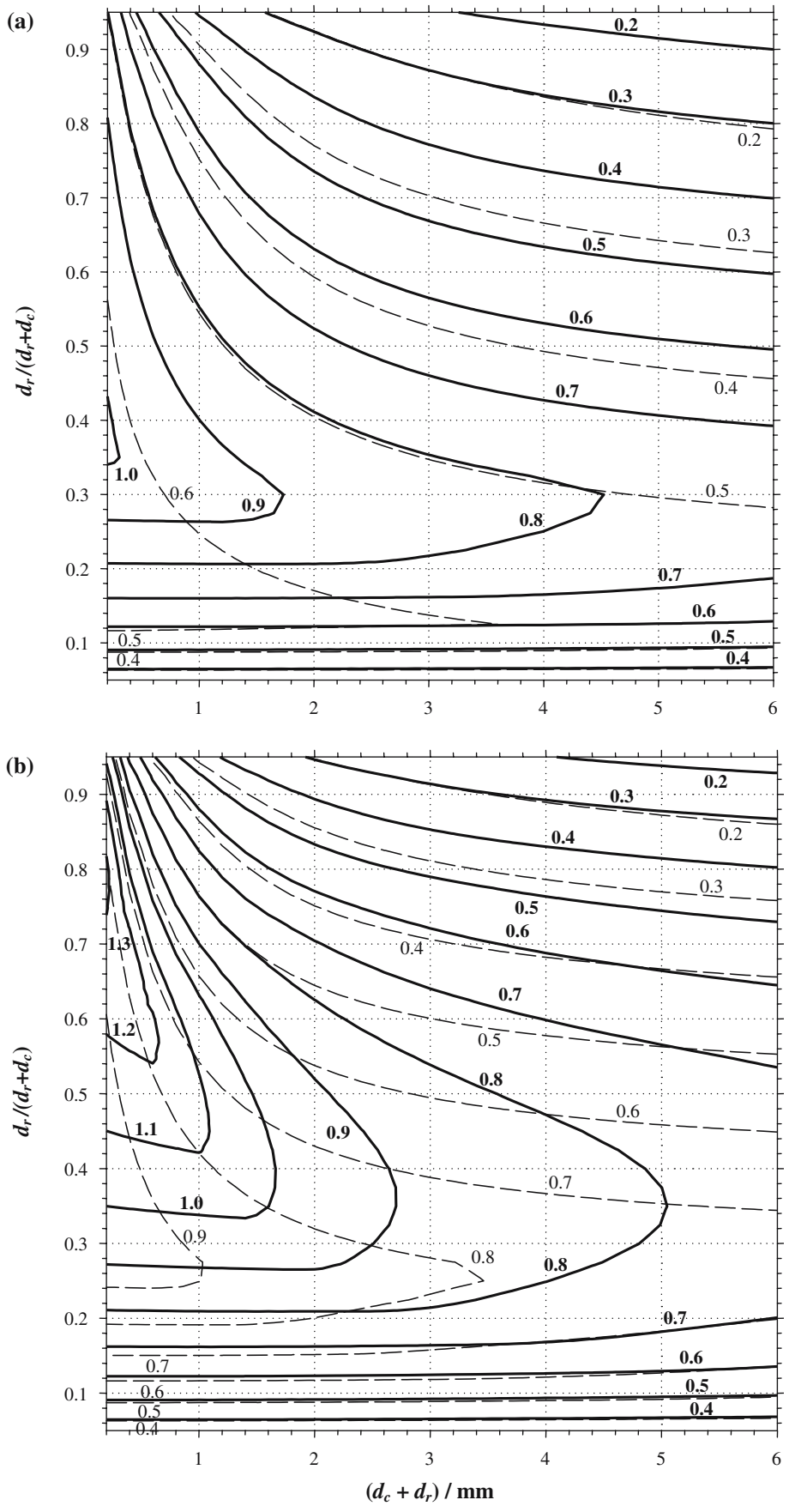

Fig. 3. Numerically calculated lines of equal values of current density (A cm^{-2}) for different gas diffusion layer thickness h (mm) and porosity ε. Thickness of membrane is 0.05 mm. Cell output voltage 0.7 V. Relative humidity of hydrogen 95%, relative humidity of air 50%. (a) Broken line – $h = 0.45$ mm, $\varepsilon = 0.5$; full line – $h = 0.45$ mm, $\varepsilon = 0.7$. (b) Broken line – $h = 0.28$ mm, $\varepsilon = 0.5$; full line – $h = 0.28$ mm, $\varepsilon = 0.7$.

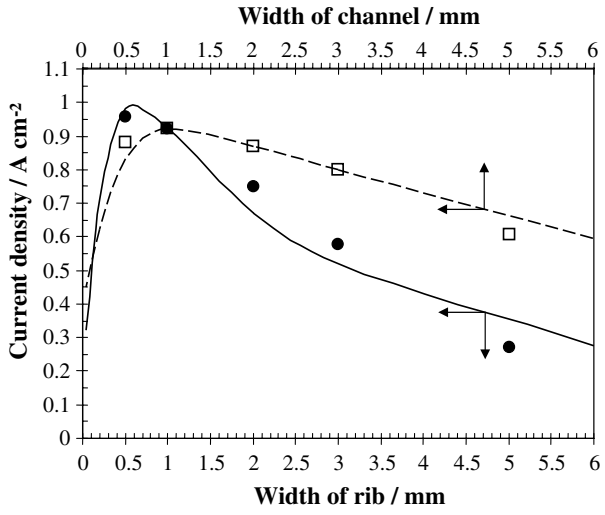

Fig. 4. Dependencies of current density on width of rib d_r (at $d_c = 1$ mm) and on width of channel d_c (at $d_r = 1$ mm) for $t = 85°C$, $Pair = 3$ bar, $PH_2 = 2$ bar, $U_{out} = 0.7$ V, $h = 0.28$ mm, $\varepsilon = 0.7$; lines – numerical results; points – experimental data: □ i vs. d_c and ● i vs. d_r.

bipolar plate (width of channels and ribs) for various gas diffusion layer parameters (thickness, effective porosity) were calculated (see Figure 3(a), (b)).

Increase in gas diffusion layer porosity from 0.5 up to 0.7 at constant gas diffusion layer thickness (0.45 mm) and cell output voltage (0.7 V) results in an increase in the optimum $d_r/(d_r + d_c)$ value (for example, from 0.15 to 0.30 at $d_r + d_c = 1$ mm, see Figure 3(a)). The same effect is observed for a thinner gas diffusion layer (0.28 mm). For example the optimum $d_r/(d_r + d_c)$ is changed from 0.27 up to 0.50 at $d_r + d_c = 1$ mm, see Figure 3(b). In addition, further decrease in $d_r + d_c$ with simultaneous increase in $d_r/(d_r + d_c)$ (to 0.78 in limiting case) produces a current density increase (up to 1.3 A cm^{-2}, see Figure 3(b)).

Generally, the model calculations show that among the considered options, the gas diffusion layer with thickness of 0.28 mm and porosity 0.7 gives the best performance. Thus, in order to reach the maximum current density it is necessary to decrease $d_r + d_c$ while keeping $d_r/(d_r + d_c)$ tending to the 0.8 limit (Figure 3(b)).

The analysis of the resulting data shows that, with reduction of the channel and current transfer rib dimensions, there is an increase in current density (see Figure 3(a), (b)). The reason is that reduced widths increase the rate of diffusion processes and decrease ohmic losses in the gas diffusion layer. Obviously, technological and material aspects of bipolar plate production [11, 12] determine the minimum dimensions of channels and ribs.

At a fixed $d_r + d_c$ value, a clear maximum in current density is observed depending on the $d_r/(d_r + d_c)$ value. The position of the maximum is determined by competition between two processes: diffusion and current conductivity in a gas diffusion layer. The rates of reagent and water vapor diffusion increase monotonically with reduction in the $d_r/(d_r + d_c)$ value. On the other hand, increase in $d_r/(d_r + d_c)$ decreases the ohmic losses in the gas diffusion layer. It was shown that for cathode gas diffusion layers of porosity 65% or more, ohmic losses in the latter could play a significant role with increasing channel width. However, a porosity of 30–40% is recommended for the anode gas diffusion layer since diffusion limitations for the anode are negligible and electrical conductivity plays a determining role.

It is necessary to note that the possible effect of "sagging" of the gas diffusion layer between adjacent ribs (i.e. deterioration of contact between gas diffusion and electrocatalytic layers), which can particularly occur for larger values of channel width (d_c), has not been taken into account in the modelling calculations. Also, possible deformation of the gas diffusion layer in the zones located opposite to ribs, which may occur for small width (d_r) and high hold-down clamping pressures, has not been taken into consideration. However, for normally employed d_r and d_c values these effects are insignificant.

4.2. *Verification of the model*

The dependencies of current density on d_r (at fixed d_c) and d_c (at fixed d_r) have been calculated (Figure 4) in order to estimate the correlation of the model calculations to experimental data. The same mathematical methods were used to calculate these dependencies (it is also possible to obtain dependencies i vs. d_r and i vs. d_c directly from Figure 3(b) by means of graphical techniques).

Experimental data obtained using various bipolar plates and gas diffusion layers agree well with the calculations. In particular, the numerical data qualitatively correlate with experimental i vs. d_r data of other authors [4, 5].

Thus, both experiments and calculations on the model show the existence of optimum values of channel and rib widths of a bipolar plate, which to a substantial extent, are determined by the gas diffusion layer properties.

5. Conclusions

A physicochemical model of a PEM fuel cell was developed. The validity of the model was tested, and the calculated results proved to be consistent with experimental data.

Both model calculations and experimental data have shown that the achievement of maximum current density requires a special correlation between cell component parameters. For instance, flow-field design has to correlate with gas diffusion layer parameters. The data obtained suggests values of operating parameters and some design requirements providing an increase in PEM fuel cell efficiency.

Furthermore the methods of PEM fuel cell modelling described here may be useful for engineering of other related electrochemical systems.

References

1. J.G. Pharoah, *J. Power Sources* **144** (2005) 77.
2. X. Li and I. Sabir, *Int. J. Hydrogen Energy* **30** (2005) 359.
3. H-M. Jung, W-Y. Lee, J-S. Park and C-S. Kim, *Int. J. Hydrogen Energy* **29** (2004) 945.
4. Y-G. Yoon, W-Y. Lee, G-G. Park, T-H. Yang and C-S. Kim, *Int. J. Hydrogen Energy* **30** (2005) 1363.
5. H-M. Jung, W-Y. Lee, J-S. Park, T-H. Yang and C-S. Kim, *Electrochim. Acta* **50** (2004) 709.
6. S.A. Grigor'ev, Yu.R. Alanakian, V.N. Fateev and V.D. Rusanov, *Doklady Phys. Chem.* **382** (2002) 31.
7. S.A. Grigor'ev, A.A. Kalinnikov, V.I. Porembskii, I.E. Baranov, E.V. Borisova and V.N. Fateev, *Russ. J. Electrochem.* **40** (2004) 1188.
8. A.A. Kulikovsky, *Numerical Methods Programming* **3** (2002) 150.
9. A. Rowe and X. Li, *J. Power Sources* **102** (2001) 82.
10. N.P. Siegel, M.W. Ellis, D.J. Nelson and M.R. von Spakovsky, *J. Power Sources* **128** (2004) 173.
11. A. Hermann, T. Chaudhuri and P. Spagnol, *Int. J. Hydrogen Energy* **30** (2005) 1297.
12. J.S. Cooper, *J. Power Sources* **129** (2004) 152.